The Micellar Cubic Phases of Lipid-Containing Systems: Analogies with Foams, Relations with the Infinite Periodic Minimal Surfaces, Sharpness of the Polar/Apolar Partition

Vittorio Luzzati, Hervé Delacroix, Annette Gulik

The Micellar Cubic Phases of Lipid-Containing Systems: Analogies with Foams, Relations with the Infinite Periodic Minimal Surfaces, Sharpness of the Polar/Apolar Partition

Vittorio Luzzati (*), Hervé Delacroix and Annette Gulik

Centre de Génétique Moléculaire, CNRS, 91198 Gif-sur-Yvette, France

(Received 19 September 1995, received in final form 9 November 1995, accepted 15 November 1995)

PACS.64.60.My – Metastable phases
PACS.64.70.Md – Transitions in liquid crystals
PACS.68.35.Md – Surface energy; thermodynamics properties

Abstract. — Of the 7 cubic phases clearly identified in lipid-containing systems, 2 are bicontinuous, 4 micellar. 3 of these are of type I: one (Q^{223}) consists of two types of micelles, the two others of identical quasi-spherical micelles close-packed in the face-centred (Q^{225}) or the body-centred mode (Q^{229}). These structures, much like foams, can be described as systems of space-filling polyhedra: distorted 12- and 14-hedra in Q^{223}, rhombic dodecahedra in Q^{225}, truncated octahedra in Q^{229}. In foams the geometry of the septa and of their junctions are generally assumed to obey Plateau's conditions, at least at vanishing water content: these conditions are satisfied in Q^{223}, can be satisfied in Q^{229} by introducing subtle distortions in the hexagonal faces, but cannot be satisfied in Q^{225}. Alternatively, these structures can be represented in terms of infinite periodic minimal surfaces (IPMS) since it is found that two types of IPMS, F-RD in Q^{225} and I-WP in Q^{229}, almost coincide with one particular equi-electron-density surface of the 3D electron density maps. These IPMS partition 3D space into two non-congruent labyrinths: in the case of the lipid phases one of the labyrinths contains the hydrated micelles, the other is filled by water. If interfacial interactions are associated with these surfaces, then the surfaces being minimal, the interactions may also be expected to be minimal. Another characteristic of the micellar phases is that the dimensions of their hydrophobic core, computed assuming that headgroups and water are totally immiscible with the chains, often are incompatible with the fully extended length of the chains. This paradox is evaded if headgroups and chains are allowed to be partially miscible with each other.

Résumé. — Des 7 phases cubiques clairement identifiées dans les systèmes lipidiques, 2 sont bicontinues, 4 micellaires. Parmi ces dernières, 3 sont du type I : une (Q^{223}) comporte deux types de micelles, deux autres sont formées de micelles identiques quasi-sphériques, empaquetées selon le mode face-centré (Q^{225}) ou centré (Q^{229}). Tout comme les mousses, ces structures peuvent être décrites en termes d'assemblages denses de polyhèdres : 12-hèdres et 14-hèdres déformés dans Q^{223}, dodecahèdres rhombiques dans Q^{225}, octahèdres tronqués dans Q^{229}. Dans les mousses la géométrie des faces et de leurs jonctions est censée obéir aux conditions de Plateau, du moins aux faibles teneurs en eau : ces conditions sont satisfaites dans Q^{223}, peuvent être satisfaites dans Q^{229} au prix d'une petite distortion des faces hexagonales, mais il est impossible de les satisfaire dans Q^{225}. On peut également représenter ces structures en termes de surfaces minimales périodiques et infinies (IPMS) : on trouve, en effet, que deux types de IPMS, F-RD pour Q^{225} et I-WP

(*) Author for correspondence

pour Q^{229}, coincident avec l'une des surfaces d'égale densité électronique des cartes 3D. Ces IPMS partagent l'espace en deux labyrinthes non congruents: dans les phases micellaires un de ces labyrinthes contient les micelles hydratées, l'autre l'eau. Si on associe à ces surfaces des interactions interfaciales, on peut alors penser que ces interactions sont minimales puisque les surfaces sont minimales. Une autre caractéristique des phases micellaires est que le rayon de leur noyau apolaire, déterminé en faisant l'hypothèse que les chaînes paraffiniques sont totalement immiscibles avec les têtes polaires et l'eau, dépasse souvent la longueur des chaînes étirées. On peut éviter ce paradoxe en admettant que chaînes et têtes polaires sont partiellement miscibles entre elles.

1. Introduction

Since our 1993 review of the cubic phases of lipid-containing systems [1] two more phases of this class have been identified and their structure shown to be micellar (Q^{225} and Q^{229} [2]). This brings to six the number of cubic phases whose structure, in our opinion, is firmly established [1,3]: four are micellar (Q^{223}, Q^{225}, Q^{227}, Q^{229}), two bicontinuous (Q^{224}, Q^{230}). A seventh phase (Q^{212}), observed so far in only one protein-lipid-water system, has been described in terms of a 3D network of lipids in which are enclosed the protein molecules [4]. Regarding the bicontinuous structure (P-type IPMS) often proposed for a phase of space group Im3m, we have repeatedly expressed the view that its very existence lacks so far firm experimental support [1,3].

One of the micellar phases (Q^{227}) consists of two types of quasi-spherical micelles (one of symmetry $\bar{3}$m, the other of symmetry $\bar{4}$3m); the space group is Fd3m [5,6]. From the chemical viewpoint this phase has been observed in systems containing a mixture of lipid molecules, heterogeneous with respect to headgroup polarity. All the known examples of this phase are of type II (water-containing micelles embedded in a hydrocarbon matrix). The structure, moreover, is related to one of the two most common types of water clathrates [1,5].

The three other micellar phases are of type I (hydrocarbon micelles embedded in a water matrix) and have all been observed in systems whose lipid component is chemically homogeneous. One of these phases (Q^{223}, space group Pm3n) contains two types of micelles, one quasi-spherical (symmetry m3), the other slightly flattened (symmetry $\bar{4}$2m); the structure is related to another common type of water clathrates [5,7,8]. Another phase (Q^{225}) has been observed in the system $C_{12}EO_{12}$-water [9] and in two ganglioside-water systems [2]. The structure consists of identical quasi-spherical micelles (symmetry m3m) close-packed in the face-centred mode (space group Fm3m) [2]. Finally, one phase of cubic aspect #8 (Q^{229}) has been observed in the system $C_{12}EO_{12}$-water [9] and in a ganglioside-water system [2]; its structure consists of identical quasi-spherical micelles (symmetry m3m) close-packed in the body-centred mode (space group Im3m) [2].

We discuss in this paper several physical and crystallographic properties of the three micellar phases of type I, whose structure we envisage from different viewpoints: as densely-packed systems of rigid spheres, as foam-like assemblies of space-filling polyhedra, as infinite periodic minimal surfaces (IPMS). We also discuss the chemical properties of the phases, with special emphasis on the notions of structure elements and of polar/apolar partition.

2. Physical and Crystallographic Properties

We may consider several facets of the structure of these micellar phases.

2.1. PACKING OF RIGID SPHERES. — The face-centred mode of space group Q^{225} is the closest 3D periodically-ordered packing of identical rigid spheres; the volume fractional coverage is 0.7405. The body-centred mode of space group Q^{229} is the second closest cubic packing, with a volume fractional coverage of 0.6801.

Different parameters can be used to assess the dimensions of the lattice and of the micelles. One is the radius of the closely packed rigid spheres, $R_{\text{c.p.}}$. the value of this parameter is defined by the symmetry of the lattice and the cell parameter. Another parameter, specified by the chemical and the crystallographic data, is the radius R_{par} of the hydrophobic core of the micelles [2]. The values of these two radii are reported in Table I. Note that in the two lipids and in the different phases the volume fraction occupied by the hydrocarbon chains ($c_{\text{v,par}}$), and consequently the ratio $R_{\text{c.p.}}/R_{\text{par}}$ are almost constant, in spite of the widely different polar/apolar ratio (the ratio $n_{\text{pol}}/n_{\text{par}}$, where n_{pol} and n_{par} are the number of electrons of the polar and the hydrocarbon moieties, is equal to 2.24 in GM1, to 4.62 in GM1(acetyl), see Tab. I in [2]).

A third parameter, relevant to the dilute micellar solutions, is the hydrodynamic radius R_{H} (also called the Stokes radius), defined operationally by light scattering and hydrodynamic experiments [10] (see Tab. I). Larger differences are observed in the Stokes radii of the two lipids, that mirror the different size of the micelles in the two experimental conditions. We return to this point in Section 3.2.

Phase Q^{223}, that contains two types of micelles, does not lend itself to this kind of analysis.

2.2. SPACE-FILLING POLYHEDRA: AN ANALOGY WITH FOAMS. — As we have pointed out earlier [2] phases Q^{223}, Q^{225} and Q^{229} can be visualized as assemblies of space-filling polyhedra. The polyhedra are rhombic dodecahedra in phase Q^{225}, truncated octahedra in phase Q^{229}, a mixture of distorted dodecahedra and tetradecahedra (in the ratio 1 to 3) in phase Q^{223} (see Fig. 1). The same polyhedra, and their space-filling assemblies, are sometimes evoked in the study of foams. Although the micellar cubic phases do not meet the usual criteria of foams ("We consider foams broadly as dispersions of gas in liquid...." [11]), we shall stretch the definition and visualize these phases as *monodisperse* foams of paraffin in water, or more precisely as assemblies of paraffin-filled cells separated from each other by water septa coated by the polar headgroups of the lipid molecules. The water content is variable in the systems considered in this paper.

In foams the geometry of the septa and of their junctions are generally assumed to obey Plateau's conditions at the limit of vanishing water content: three faces join at each edge with mutual angles equal to 120°; four edges meet at each vertex with mutual angles equal to 109°28′. As the water content increases, these constraints are expected to relax. According to Wearie and Pheland [12] the lowest surface energy at the limit of vanishing water content corresponds to the body-centred packing of Kelvin's tetrakaidecahedra. These space-filling polyhedra, with eight hexagonal and six quadrilateral faces, derive from the regular truncated octahedra by a subtle distribution of curvature on the hexagonal faces: this distortion has the effect of bringing the angles at the vertices (that are of 120° and 90° in the truncated octahedron) closer to tetrahedral [12]. At higher water content the lowest surface energy seems to correspond to the clathrate-like space-filling assembly of dodecahedra and tetradecahedra (phase Q^{223}). In this structure, it must be stressed, the faces meet at angles close to 120° and each vertex is a quasi-regular tetrahedral junction of four edges [13]. At still higher water content the lowest surface energy seems to correspond to a system of regular rhombic dodecahedra packed in the face-centred cubic mode, much like the micellar phase Q^{225}. This last structure falls short of fulfilling Plateau's conditions: four edges join tetrahedrally at eight of the vertices of each rhombic dodecahedral cell but eight edges join octahedrally at the six other vertices.

Table I. — *Dimensions of the structure elements. The crystallographic and chemical data correspond to the experiments reported in [2]. c_v is the volume concentration (lipid/lipid+water). a is the parameter of the cubic cell, $c_{v,par}$ is the volume concentration of the apolar moiety. According to the micellar interpretation the structure consists of disjointed micelles: ν is the number of micelles per unit cell, $R_{c\,p}$ is the radius of the close packed spheres (equal to 0.354a for the face-centred, to 0.433a for the body-centred packing). $N_{agg} = a^3/(\nu v_{vol})$ is the number of lipid molecules in one micelle, where v_{vol} is the volume of one lipid molecule (see Tab. I in [2]); R_{par} and $(S_{mol})_{sph}$ are the radius of the paraffin core of the micelles, supposed to be spherical and the area-per molecule at the surface of the paraffin core, $(S_{mol})_{polyh}$ is the area per molecule at the surface of the paraffin core supposed to be polyhedral (see Eq. (2)). Since phase Q^{223} contains two types of micelles the dimensions (printed in italics) are average values. According to the IPMS interpretation the structure consists of two non-congruent labyrinths, separated by an IPMS: φ_F and φ_I are the fractional volume coverage of the F- and the I-labyrinths: $(S_{mol})_{IPMS} = \sigma a^2/(\nu N_{agg})$ is the area-per-molecule at the IPMS, $(\lambda_{mol})_X = \varphi_X a^3/(\nu v_{mol} N_{agg})$ is the volume ratio (X-labyrinth)/(lipid molecules). R_g is the average Gaussian radius of curvature of the IPMS (Eqs. (7) and (8)). $\eta_{sugar} = (\lambda_{mol}^{-1})v_{mol}/(v_{mol} - v_{par})$ is the apparent hydration of the sugar moiety (Eq. (9)). # In this experiment the water was buffered at pH 7 (citrate 0.1 M).*

crystallographic and chemical data							
experiment		A	B	C	D	E	F
lipid		GM1	GM1	GM1	GM1 (ac)	GM1 (ac)	GM1 (ac)
medium		H_2O	H_2O-gly	H_2O-gly	H_2O#	H_2O	H_2O
T	(°C)	20	20	70	20	20	20
c_v		0.288	0.283	0.274	0.461	0.461	0.461
phase		Q^{225}	Q^{225}	Q^{223}	Q^{225}	Q^{225}	Q^{229}
a	(Å)	155	147	187	123	108	85

micellar interpretation							
ν		4	4	8	4	4	2
$R_{c\,p}$	(Å)	54.8	52.0		43.5	38.2	36.8
N_{agg}		128	107	107	131	88	86
$c_{v\,par}$		0.128	0.126	0.122	0.133	0.133	0.133
R_{par}	(Å)	30.5	28.8	*28.8*	24.5	21.5	21.4
$(S_{mol})_{sph}$	(Å^2/mol)	91.2	97.4	*97.4*	57.6	66.6	66.9
$(S_{mol})_{polyh}$	(Å^2/mol)	101.4	107.0	106.1	64.2	73.3	73.3

IPMS interpretation							
IPMS		F-RD	F-RD	-	F-RD	F-RD	I-WP
φ_F, φ_I		0.532	0.532	-	0.532	0.532	0.536
$(S_{mol})_{IPMS}$	(Å^2/mol)	141.1	151.8	-	86.8	99.6	115.5
λ_{mol}		1.85	1.88	-	1.15	1.15	1.16
R_g	(Å)	33.9	32.2	-	26.9	23.6	30.0
η_{sugar}		1.53	1.58		0.21	0.21	0.22

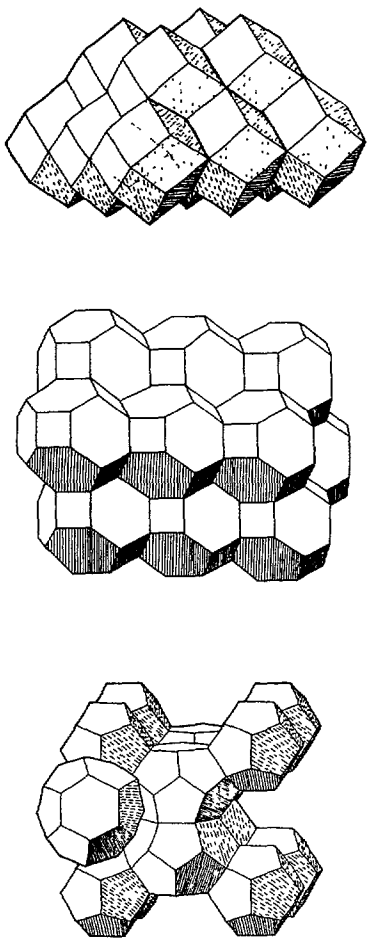

Fig. 1. — Space-filling packings of polyhedra relevant to the micellar cubic phases discussed in the text. *Upper frame*: f.c.c. packing of regular rhombic dodecahedra (phase Q^{225}, space group Fm3m). *Middle frame*: b.c.c. packing of regular truncated octahedra (phase Q^{229}, space group Im3m). *Lower frame*: p.c. packing of distorted dodecahedra and tetradecahedra (phase Q^{223}, space group Pm3n). Reproduced or redrawn, with permission, from [26].

The structure of the three micellar cubic phases [2] and their sequence $Q^{223} \Rightarrow Q^{229} \Rightarrow Q^{225}$ as a function of increasing water content [2, 9] are consistent with these theoretical expectations, although phase Q^{223} seems to be more stable than phase Q^{229} at lower water content.

For the three types of structure Wearie and Phelan [12] have tabulated the value of the "isoperimetric quotient" ζ, a parameter proportional to the dimensionless ratio V^2/S^3, where V and S are the volume and surface area (the average area in the case of the clathrate-like structure):

$$\zeta = 36\pi V^2/S^3 \tag{1}$$

The surface/volume ratio is a simple expression of ζ:

$$S/V = (1/a)[(36\pi\nu)/(\zeta\varphi)]^{1/3} \tag{2}$$

where φ is the volume fractional coverage (in this case, the volume concentration) of the micelles, ν is the number of micelles per cubic cell, a is the parameter of the cell. ν and ζ are respectively 8 and 0.764 for Q^{223}, 4 and 0.7405 for Q^{225}, 2 and 0.757 for Q^{229}. Assuming that the micelles contain the apolar moiety of the lipid molecules (i.e. $\varphi = c_{v,par}$) the average area available to one lipid molecule at the surface of the micelles is:

$$S_{mol} = (S/V)v_{par} \tag{3}$$

where v_{par} is the volume of the hydrocarbon moiety of one lipid molecule [2]. The values of S_{mol} relevant to spherical and polyhedral micelles are reported in Table I.

2.3. Infinite Periodic Minimal Surfaces. — The IPMS are surfaces of vanishing mean curvature that partition space into two disjointed 3D labyrinths. For over a century these surfaces have been the object of mathematical studies [14, 15]; more recently, the IPMS have found a variety of physical and chemical applications [16].

In order to sketch the layout and the connectivity of the labyrinths it is expedient to refer to the skeletal graphs, namely to the systems of connected edges that follow the core of the labyrinths [15].

The relevance of the IPMS to the bicontinuous cubic phases of lipid-containing systems stems from the fact that these phases can be thought of as lipid bilayers folded in space according to an IPMS: D-surface in phase Q^{224}, G-surface in phase Q^{230}, P-surface in phase Q^{229} The two labyrinths are directly congruent in phases Q^{224} and Q^{229}, chirally congruent in phase Q^{230} The skeletal graphs of these surfaces coincide with the 3-, 4- and 6-connected systems of rods that are commonly used in the structural description of phases Q^{230}, Q^{224} and Q^{229} [1]. The centre of the bilayer, whose locus is the minimal surface, and the skeletal graph reside respectively in the polar and in the apolar region if the structure is of type I, the other way around if the structure is of type II.

In contrast the micellar cubic phases, that subdivide 3D space into an infinite number of disjointed compartments of one polarity embedded in a matrix of the opposite polarity, are by no means bicontinuous. One might thus expect these phases to be utterly unrelated with the IPMS. This is certainly the case for those IPMS whose labyrinths are congruent: the issue is not as clear-cut for those IPMS whose labyrinths are not congruent. In particular two of the IPMS, I-WP and F-RD [15], display striking correlations with the micellar cubic phases Q^{229} and Q^{225} These two surfaces can be visualized by reference to the polyhedra of Figure 1 and to the pair of non-congruent skeletal graphs.

Regarding the I-WP surface, one of the graphs (I-graph) is constructed by joining with straight lines all nearest neighbour points of the b.c.c. lattice: the lines are 8-connected at

---

Fig. 2. — **(To be seen in landscape)** Composite representation of the electron density maps and of the IPMS. *Black lines*: sections through the origin of the function $\Delta\rho(\mathbf{r}) = [\rho(\mathbf{r}) - \langle\rho\rangle]/\{\langle[\rho(\mathbf{r}) - \langle\rho\rangle]^2\rangle\}^{1/2}$ ($\langle\rho(\mathbf{r})\rangle$ is the average of $\rho(\mathbf{r})$ over the volume of the cell), parallel to the planes [100], [110] and [111]; the interval between isodensity lines is 0.5; 0 and positive lines full, negative lines dotted (from Fig. 6 of [2]). *Red Lines*: traces of the IPMS, computed using equations (4) to (6). *Blue and green lines*: skeletal graphs corresponding respectively to the predominantly apolar and polar labyrinths. *Green areas*: sections of the polar labyrinths. **Left**: phase Q^{225} of GM1 (experiment A of [2]); the IPMS is the F-RD surface, the F-graph is blue, the RD-graph green. **Right**: phase Q^{229} of GM1(acetyl) (experiment F of [2]); the IPMS is the I-WP surface, the I-graph is blue, the PW-graph green. Note that in the two cases the IPMS coincides with one of the continuous isodensity lines. Note also that not all of the sections contain elements of the skeletal graphs. The scale bars correspond to 100 Å. ⟶

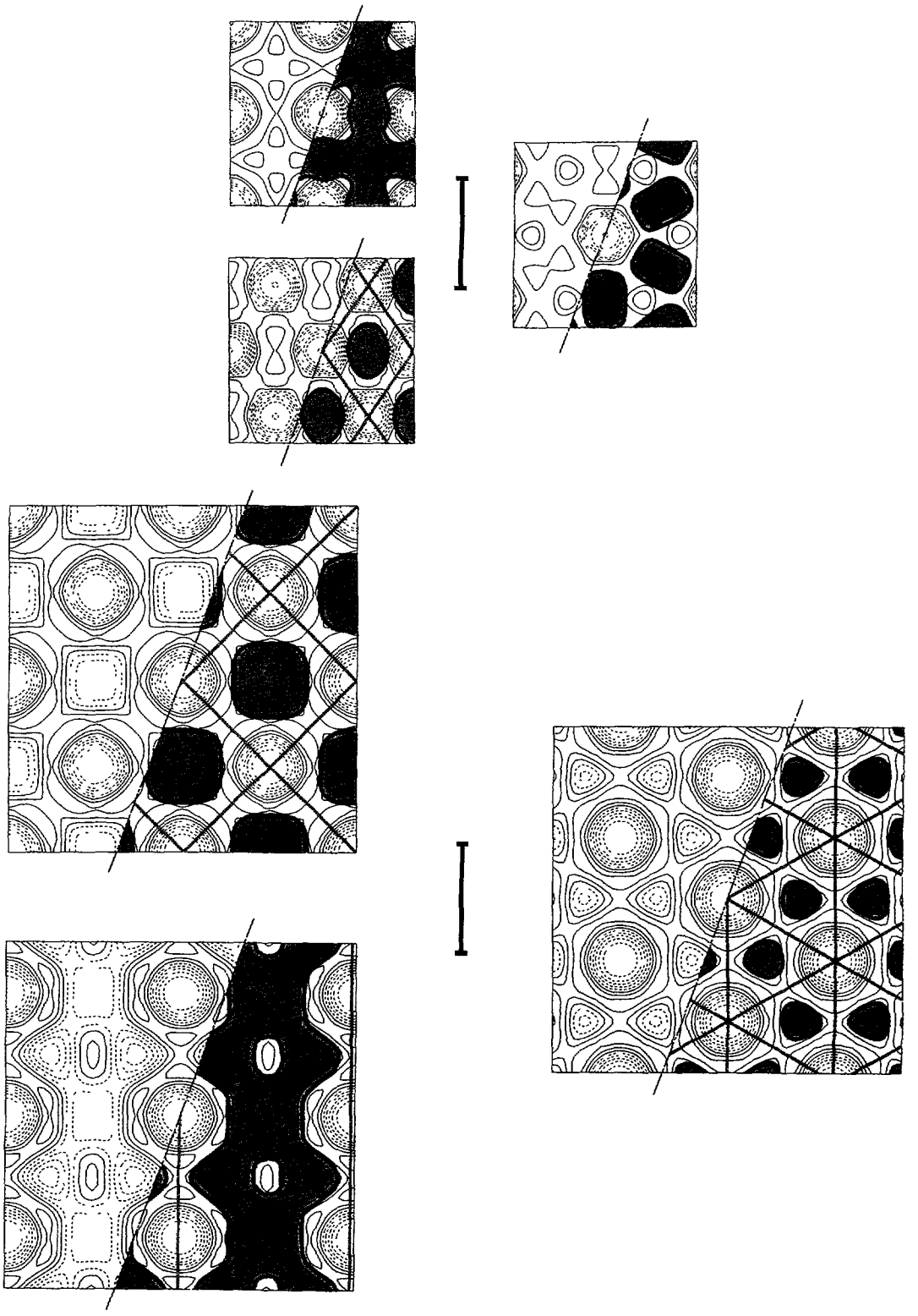

both ends. The other graph (WP-graph) is the assembly of all the edges of the space-filling assembly of regular truncated octahedra (see Fig. 1): the edges are 4-connected at both ends.

As for the F-RD surface, one of the graphs (F-graph) consists of the straight lines joining all nearest neighbour points of the f.c.c. lattice; the lines are 12-connected at both ends. The other graph (RD-graph) is the assembly of all the edges of a space-filling assembly of regular rhombic dodecahedra (Fig. 1): the edges are 4-connected at one end, 8-connected at the other.

Although the precise parametrization of these surfaces is available [17], we adopt here the nodal surface approximation advocated by von Schnering and Nesper [18]:

$$\text{I} - \text{WP} \qquad 2(\cos X \cos Y + \cos Y \cos Z + \cos X \cos Z) - (\cos 2X + \cos 2Y + \cos 2Z) = 0 \quad (4)$$

$$\text{F} - \text{RD} \qquad 4 \cos X \cos Y \cos Z - (\cos 2X \cos 2Y + \cos 2Y \cos 2Z + \cos 2X \cos 2Z) = 0 \quad (5)$$

$$X = 2\pi x, \text{etc.} \quad (6)$$

The sections [100], [110] and [111] of the two IPMS and of the corresponding electron density maps (phases Q^{229} of GM1(acetyl) and Q^{225} of GM1, [2]) are plotted in Figure 2.

A striking result emerges from Figure 2: in each of the two cases the relevant IPMS is almost coincident with one particular equi-electron-density surface. In other words, one experimentally defined surface ($\rho(\mathbf{r})$ = constant) exists whose mean curvature vanishes everywhere. This feature is reminescent of the conspicuous valleys (corresponding to the CH_3 end-groups of the chains) that groove the maps of the bicontinuous phase Q^{230}, whose bottom follows either the skeletal graph or the G-type IMPS [1]. This empirical observation aroused our suspicion that the structure of phases Q^{225} and Q^{229} might be related to the IPMS and prompted us to explore this possibility.

Several parameters relevant to these IPMS can be determined: the volume fractional coverage φ_Z of the Z labyrinth, the area per unit cell S [19]:

$$S = \sigma a^2 \quad (7a)$$

$$\sigma = H[(-2\pi\xi)^{1/2}]^{2/3} \quad (7b)$$

where ξ is the Euler-characteristic and H the "homogeneity index", a the unit cell parameter: the average Gaussian curvature γ^2 and the corresponding radius of curvature R_g:

$$\gamma^2 = -2\pi\xi/S = (R_g)^{-2} \quad (8)$$

The values of these parameters relevant to the IPMS I-WP and F-RD are [19, 20]:

IPMS	ξ	H	σ	φ_I	φ_F
I-WP	−6	0.7425	2.749	0.536	-
F-RD	−10	0.6577	3.007	-	0.532

The results are reported in Table I and discussed in Section 3.4.

3. Chemical and thermodynamic properties

3.1. Polar/Apolar Partition and the Notion of Structure Element. — The notion of structure element, that paves the way to the determination of a variety of geometric parameters, was introduced very early in the study of lipid polymorphism and widely used

since [21]. In the case of gangliosides, as we discuss below, this notion is somewhat strained. It is thus appropriate to look more closely at the underlying assumptions.

In the study of lipid-water systems it is customary to partition space into two ideal subvolumes associated with the more and the less polar moiety of the system. These volumes, whose shape and position are supposed to fulfill the crystallographic constraints (symmetry, cell dimensions, etc.) constitute the structure elements. The composition of these elements depends upon the chemical criteria used to discriminate the polar from the apolar moieties.

Several years ago, and after some hesitation, we advocated [22] to ascribe the CH, CH_2 and CH_3 groups of the hydrocarbon chains to the apolar moiety, the water and the rest of the lipid molecules to the polar medium (see, for example, Fig. 1 in [2]). This was a fortunate choice since in most of the lipid-water systems it led to area-per-chain values that increase or remain constant, but that never decrease as the water content increases, even when phase boundaries are crossed. Besides, when the polar/apolar separation is assumed to be sharp, then it follows that no point of the apolar volume can be further away from the polar/apolar interface than the fully extended length L_{max} of the longest hydrocarbon chain. This proposition has provided a handy criterion to test the validity of some structural models [23] ([1]).

In some systems, nevertheless, the decision of what portion of the lipids mixes with the hydrocarbon chains, what with water is less trivial; by way of example we may quote the soap-fatty alcohol-water phases [24] and the lipid-water phases of some Archaebacteria lipids [23]. We have approached this problem recently from a more phenomenological standpoint, based upon the proposition that in any pair of phases in thermodynamic equilibrium the area/volume ratio of the apolar structure elements is invariant [3]. Implicit in this proposition is the assumption that the polar/apolar interfacial interactions are predominant over all the other forces at play in the system. A rewarding aspect of this approach is that it yields an operational definition of the chemical composition of the structure elements, and thus of the partition between polar and apolar volumes [3]. We have applied this approach to the scores of lipid-water systems whose X-ray scattering data are reported in the literature. We have thus found that the apparent partition is highly variable from lipid to lipid: the content of the apolar structure elements varies from less than one half of the hydrocarbon chains to the whole of the lipid molecules. The partition also seems to display strong correlations with the chemical properties of the lipid molecules [3].

This is as far as one can go without forsaking the postulate that each chemical group of the system belongs entirely to one or the other type of structure elements. We introduce in next Section the notion that the separation may be less sharp and we explore the possibility that the headgroups be somewhat miscible with the hydrocarbon chains.

3.2. Micellar Interpretation: Partial Miscibility of Headgroups and Hydrocarbon Chains. — The value of the fully extended length L_{max} of a paraffin chain can be assessed from the standard dimensions of the paraffin molecules: following Tanford [25] we take the projected length of the CH_3, CH_2 and CH groups to be respectively 2.5, 1.25 and 0.95 Å. In the case of GM1 and GM1(acetyl) the longuest chain (labeled X in Fig. 1 of [2]) is respectively $-(CH_2)_{17} - CH_3$ and $-CH_3$, the other chain is $-CH = CH - (CH_2)_{12} - CH_3$. Therefore, L_{max} is equal to 25.0 Å for GM1, to 19.4 Å for GM1(acetyl).

In all the experiments (see Tab. I) the radius R_{par} of the apolar core of the micelles, assumed to be spherical, turns out to be larger than L_{max}. Although some of the differences seem to be marginal, others are significant and need be explained. One possibility is that the shape of the

([1]) A similar problem has arisen in the early crystallographic study of phase Q^{223} [4,31]. In that case, the assumption that all the micelles are spherical misled Tardieu and Luzzati into ruling out a micellar structure and putting forward a rod-and-micelle model that was later shown to be incorrect [5,7,8].

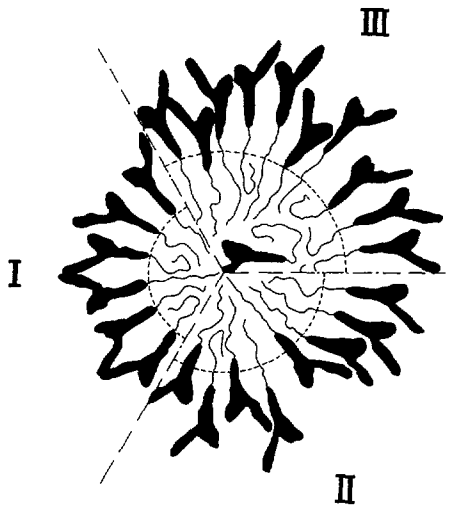

Fig. 3. — Schematic representation of an equatorial section of a spherical micelle of GM1(acetyl) [2]. The black silhouettes represent the polar headgroups, the wriggling threads the hydrocarbon chains in their disordered conformation. The two moieties are drawn at approximately the same scale. The three sectors correspond to different modes of polar/apolar segregation. The dotted circles represent the virtual spheres of radius R_{par} whose volume is equal to the volume of the hydrocarbon chains contained in the micelle. **I)** The headgroups and the hydrocarbon chains do not mix; in this case R_{par} cannot exceed the fully extended length L_{max} of the longest chain. **II)** A portion of the headgroups is in contact with the chains; in this case R_{par} may be larger than L_{max}. **III)** A fraction of the headgroups is embedded in the chains; in this case R_{par} can be much larger than L_{max}.

micelles departs from spherical. Adopting, for example, the polyhedral shape compatible with the space group (see Fig. 1) the shortest distance (from centre to face) decreases to $0.905R_{par}$ in phase Q^{225}, to $0.879R_{par}$ in phase Q^{229} [26]. As for phase Q^{223} (experiment C) the radius of the paraffin core of the micelles, that is equal to 28.8 Å if the 8 micelles of the unit cell are all identical spheres, drops to 23.1 Å if 6 of the 8 micelles are assumed to be ellipsoids of axes R_{par}. 1.5 R_{par}. 1.5 R_{par} [13] ([1]). Wrinkling the surface, a process that would formally improve the agreement, cannot be pushed very far with these small and highly symmetrical micelles without the hydrocarbon chains coming in contact with water. The conclusion is thus difficult to escape that the radius of the apolar core of the micelles is not always compatible with the fully extended length of the chains.

This anomaly stems from the assumption that the partition into polar and apolar structure elements is perfectly sharp. An obvious way to elude the paradox is to allow some of the polar headgroups to dip to some depth inside the hydrocarbon volume or a few of the headgroups to be entirely embedded in the paraffin core of the micelles, as visualized in Figure 3: in either case the constraint $R_{par} \leq L_{max}$ ceases to be peremptory.

In this respect, it is instructive to compare the dimensions of the micelles in the cubic phases with those reported in the dilute micellar solutions (Tab. II). In the case of GM1(acetyl) the number of lipid molecules per micelle is almost the same in the cubic phases Q^{225} ($N_{agg} = 88$, experiment E) and Q^{229} ($N_{agg} = 86$, experiments F); R_{par} in these experiments barely exceeds L_{max}. In solution N_{agg} takes almost the same value ($N_{agg} = 76$ [27]): Sonnino *et al.* [27] have

Table II. — *Dimensions of the micelles in the dilute micellar solutions. The aggregation number N_{agg} and the hydrodynamic (Stokes) radius R_H are from [27].*

lipid	GM1	GM1 (acetyl)
N_{agg}	301	76
R_H (Å)	58.7	34.0

indeed proposed a spherical shape for these micelles. N_{agg} and R_{par} are larger in experiment D ($N_{agg} = 131$; $R_{par} = 24.5$ Å). These parameters are still larger in the case of GM1: in the cubic phases N_{agg} and R_{par} are respectively 128 and 30.5 Å (experiment A) and 107 and 28.8 Å (experiments B and C). The conclusion is thus difficult to escape, especially in experiments A and D, that the separation between the headgroups and the hydrocarbon chains is not quite sharp. In an early study of the micellar solution of GM1 Corti *et al.* [28] have reported $N_{agg} = 301$, a value substantially larger than in any of the cubic phases. In order to reconcile the observed values of N_{agg} and of R_H with the proposition that no point of the micelle is further away from the polar/apolar interface than the fully extended length of the chains (see above) these authors resorted to a toroidal model [28]. More recently Cantú *et al.* [29] have tackled the same problem using light and small angle X-ray and neutron scattering experiments and have put forward a spherically-symmetric model containing a hydrophobic core of radius 43.4 Å. Most surprisingly, these authors passed over the substantial discrepancy of the model with the length of the chains ($L_{max} = 23$ Å) under silence. If one is to follow all of the arguments presented in that paper [29], then one can hardly escape the conclusion that in this case also the headgroups come in contact with the apolar core of the micelle, as illustrated in Figure 3.

One may expect that the space distribution of the different moieties be mirrored in the electron density maps (see Figs. 6 and 7 in [2]). It must be stressed, nevertheless, that the experimental maps refer to the unscaled electron density contrast $K[\rho(\mathbf{r})-\langle\rho\rangle]$, where K is an unknown scaling factor different in each experiment and $\langle\rho\rangle$ is the average electron density. Comparing different curves means drawing them on the same scale and with the same origin. In other words, two points of each function $\rho(\mathbf{r})$ must be determined *a priori* in absolute terms, using some independent information. One of these is $\langle\rho\rangle$, that can be determined when chemical composition and partial specific volumes are known. The choice of a second point is more problematic; the uncertainties are such that a comparison lacks all practical value.

3.3. IPMS INTERPRETATION. — The volume coverage of the F and the I labyrinths, in which the hydrophobic cores of the micelles are embedded, are much larger than the volume concentrations of the lipids (compare c_v and φ_F, φ_F in Tab. I). Hence these labyrinths must also contain water, in addition to the lipid micelles. The amount of water can be expressed in terms of hydration of the sugar moiety:

$$\eta_{sugar} = (\chi_{mol} - 1)v_{mol}/v_{sugar} \tag{9}$$

η_{sugar} is the water/sugar (volume) ratio, v_{sugar} is the volume occupied by one sugar headgroups (v_{pol} in Tab. I of [2]). The values of η_{sugar} are given in Table I.

It is noteworthy that the hydration increases as the packing density of the sugar headgroups decreases (i.e. η_{sugar} increases as $(S_{mol})_{IPMS}$ increases, see Tab. I), as if bringing the sugar headgroups closer together should have the effect of squeezing out some of the water.

4. Discussion and Conclusions

The possibility that some of the headgroups be somewhat miscible with the hydrocarbon chains has been considered in the past, but only in circumstances in which the headgroups were highly heterogeneous [1, 23, 24]. One novelty of this work is to evoke this possibility in lipid-water systems in which the lipid component is chemically homogeneous. In operational terms, the anomaly observed in some of the micellar cubic phases - and only in phases of this type - is that the fully extended length of the chains fails to meet the dimensions of the micelles, at least as long as chains and headgroups are assumed to be totally immiscible with each other. The presence of some miscibility suffices to evade this paradox. In keeping with this miscibility, note that the headgroups of $C_{12}EO_{12}$ [9] and gangliosides [2] (the only lipids known so far to display the micellar phases Q^{229} and Q^{225}) are exceptionally bulky and flexible, and also somewhat soluble in hydrocarbons.

It must also be noted that phases belonging to space groups N° 225 and 229, along with the bicontinuous phases Q^{224} and Q^{230}, have been reported in a variety of three-component systems (didodecylammonium bromide)-water-hydrocarbon oil [30].

Another novelty of this work is to involve the IPMS in the analysis of the micellar cubic phases: the IPMS have indeed been evoked in the past only in the context of the bicontinuous cubic phases. The reference to the IPMS stems from the empirical observation, documented in Figure 2 and discussed in Section 2.3, that in two of the phases the corresponding IPMS (F-RD for Q^{225}, I-WP for Q^{229}) coincides with one particular equidensity surface of the 3D electron density map. This remarkable observation hints at some subtle correlation between the structure of the phases and the IPMS. We may discuss the possible nature of this correlation and attempt to reconcile the IPMS with the more conventional description in terms of space-filling polyhedra.

Let us first consider phase Q^{223}, the least hydrated [9], and apparently the most common [7, 8, 31] of the micellar phases of type I. The structure can be described in terms of space-filling distorted dodecahedra and tetradecahedra (Sect. 2.2). The angles between joining faces and joining edges are all close to respectively 120° and 109°28′: thus, if the thickness of the interstitial layer between the micelles is negligible, then Plateau's conditions are fulfilled and the system behaves as a dry foam [12]. It must be stressed nevertheless that the analogy with foams requires that the physical objects at whose surface the interfacial forces are supposed to apply consist of highly hydrated micelles.

The next phase in the order of increasing water content is Q^{229} [2, 9]. In terms of space-filling polyhedra this phase cannot be built using regular polyhedra without the angles being seriously at variance with Plateau's conditions. As discussed in [12] one way to decrease the interfacial energy is to buckle the surface of the polyhedra, transforming the truncated octahedra into Kelvin's tetrakaidecahedra. As in the case of phase Q^{223} the objects at whose surface the interfacial forces are supposed to apply are highly hydrated micelles. Alternatively, the interfacial forces can be supposed to apply at the I-WP surface: since this surface is minimal, then the interfacial energy is also minimal. It must be stressed that the virtual I-WP surface separates a 3D labyrinth filled by water from another labyrinth formed by the highly hydrated micelles fused together *via* their hexagonal faces.

As for phase Q^{225}, whose structure consists of space-filling regular rhombic dodecahedra (Sect. 2.2), the angles between faces and edges fall short of meeting Plateau's conditions. As in the case of phase Q^{229} one way to minimize the interfacial energy is to apply the interfacial forces to the virtual F-RD surface that separates a water-filled 3D labyrinth from another labyrinth of hydrated micelles fused together *via* their quadrilateral faces.

In the last two cases (phases Q^{229} and Q^{225}) the volume ratio of the two labyrinths is fixed and their content is defined by the chemical composition of the system. Presumably, in order that the IPMS representation make physical sense the size and shape of the labyrinths must be such that water, paraffins and headgroups properly fit together, the headgroups of different micelles neatly interlock across the merging faces and present a smooth surface at the interface. All these conditions are not easy to meet: this may be the reason why the micellar cubic phases Q^{229} and Q^{225} are so rare in lipid-water systems.

In conclusion, one may conjecture that the space-filling polyhedra do not always provide the best solution of the problem of minimizing interfacial energy. The solution offered by the IPMS might sometimes be more satisfactory, at least as long as the chemical composition complies with the strict geometric constraints. When these conditions are all met, then the size of the micelles and their arrangement in space set the boundary conditions (lattice dimensions and symmetry) of the IPMS.

From a formal viewpoint the reference to the IPMS, much like the recent proposition that any two phases in thermodynamic equilibrium consist of structure elements with the same area/volume ratio [3], emphasizes the rôle of the interfacial interactions in the stability of lipid-water phases.

References

[1] Luzzati V., Vargas R., Mariani P., Gulik A. and Delacroix H., *J. Mol. Biol.* **229** (1993) 540-551.

[2] Gulik A., Delacroix H., Kirschner G. and Luzzati V., *J. Phys. II France* **5** (1995) 445-464.

[3] Luzzati V., *J. Phys. II France* **5** (1995). 649-1669.

[4] Mariani P., Delacroix H. and Luzzati V. *J. Mol. Biol.* **204** (1988) 165-189.

[5] Charvolin J. and Sadoc J.F., *J. Phys. II France* **49** (1988) 521-526.

[6] Luzzati V., Vargas R., Gulik A., Mariani P., Seddon J.M. and Rivas E., *Biochemistry* **31** (1992) 279-285.

[7] Fontell K., Fox K. and Hansson E., *Mol. Cryst. Liq. Cryst.* **1** (1985) 9-17.

[8] Vargas R., Mariani P., Gulik A. and Luzzati V., *J. Mol. Biol.* **225** (1992) 137-145.

[9] Mirkin R. J., Ph D Thesis (1992), University of Southampton, UK.

[10] Tanford C., Physical Chemistry of Macromolecules (Wiley, New York, 1961).

[11] Hansen R.S. and Derderian E.J., in "Foams", R.J. Akers Ed. (Academic Press, New York, 1976) pp. 1-16.

[12] Wearie D., *Phil. Mag. Lett.* **69** (1994) 99-105; Wearie D. and Phelan R., *Philos. Mag. Lett.* **69** (1994) 107-110.

[13] McCullan R. K. and Jeffrey G. A., *J. Chem. Phys.* **42** (1965) 2725-2732.

[14] Schwarz H.A., Gesammelte Mathematische Abhaldungen, Vol. 1 (Springer, Berlin 1880); "International Workshop on Geometry and Interfaces", E. Dubois-Violette and B. Pansu Eds., *J. Phys. Colloq. France* **51**, C7 (1990).

[15] Schoen A.H., Infinite periodic minimal surfaces without intersections, NASA Technical Note D-5541, Washington DC (1970).

[16] Andersson S. and Hyde S.T., *Angew. Chemie* **95** (1983) 67; Hyde S.T., in "Defects and processes in the solid state: geoscience applications. The McLaren Volume", J.L. Boland and J.D. Fitz Gerald Eds. (Elsevier Science Publishers, Amsterdam 1993) pp 317-342; von Schnering H.G. and Nesper R., *Angew. Chemie* **26** (1987) 1059-1080.

[17] Fogden A., *J. Phys. I France* **2** (1992) 233-239; Lidin S., Hyde S.T. and Ninham B.W., *J. Phys. France* **51** (1990) 801-813.
[18] von Schnering H. G. and Nesper R., *Z. Phys. B Cond. Matter* **83** (1991) 407-412.
[19] Engblom J. and Hyde S.T., *J. Phys. II France* **5** (1995) 171-190.
[20] Anderson D.M., PhD Thesis (1986), University of Minbnesota, USA.
[21] Luzzati V., in "Biological Membranes", D. Chapman Ed. (Acad. Press, New York 1968) pp. 71-123.
[22] Luzzati V., Tardieu A., Gulik-Krzywicki T., Rivas E. and Reiss-Husson F., *Nature* **220** (1968) 485-488.
[23] Gulik A., Luzzati V., DeRosa M. and Gambacorta A., *J. Mol. Biol.* **182** (1985) 131-149; Gulik A., Luzzati V., DeRosa M. and Gambacorta A., *J. Mol. Biol.* **201** (1988) 429-435.
[24] François J., Gilg B., Spegt P.A. and Skoulios A.E., *J. Coll. Interf. Sci.* **21** (1966) 293-314.
[25] Tanford C., The Hydrophobic Effect: Formation of Micelles and Biological Membranes (John Wiley & Sons, New York, 1980).
[26] Williams R., The geometrical foundation of natural structures (Dover Publ., New York, 1979).
[27] Sonnino S., Cantú L., Corti M., Acquotti D, Kirschner G. and Tettamanti G., *Chem. Phys. Lip.* **56** (1990) 49-57.
[28] Corti M., Cantú L. and Sonnino S., in "Gangliosides and modulation of neural functions",H. Rahmann Ed., NATO ASI Series, Vol. H7 (Springer-Verlag, Berlin, 1987) pp 101-118.
[29] Cantú L., Corti M., Zemb T. and Williams C., *J. Phys. IV France* **3** (1993) C8-221-227.
[30] Barois P., Eidam D. and Hyde S. T., *J. Phys. Colloq. France* **51** (1990) 25-34; Maddaford P. J. and Topragcioglu C., *Langmuir* **3** (1993) 2868-2878.
[31] Tardieu A. and Luzzati V., *Biochim. Biophys. Acta* **219** (1970) 11-17.